Silicene Quantum Dots: Synthesis, Spectroscopy and Electrochemical Studies

*Peiguang Hu, Limei Chen, Jia-En Lu, Hsiau-Wei Lee, and Shaowei Chen**

Department of Chemistry and Biochemistry, University of California, 1156 High Street, Santa Cruz, CA 95064

ABSTRACT

Organically functionalized silicene quantum dots (SiQDs) were synthesized by chemical exfoliation of calcium silicide and stabilized by hydrosilylation with olefin/acetylene derivatives forming Si-CH_2-CH_2- or Si-CH=CH- interfacial bonds. TEM and AFM measurements showed that the resultant SiQDs were *ca*. 2 nm in diameter and consisted of *ca*. 4 atomic layers of silicon. The structure was further characterized by ^{1}H and ^{29}Si NMR and XPS measurements. In photoluminescence measurements, the SiQDs exhibited a strong emission at 385 nm and the intensity varied with the interfacial linkage. In electrochemical measurements, both ethynylferrocene- and vinylferrocene-functionalized SiQDs exhibited a pair of well-defined voltammetric peaks at +0.15 V (vs Fc^+/Fc) in the dark for the redox reaction of the ferrocene/ferrocenium couple; yet under UV photoirradiation, an additional pair of voltammetric peaks appeared at −0.41 V, most likely due to the electron-transfer reaction of ferrocene anions formed by photoinduced electron transfer from the SiQD to the ferrocene metal centers.

Introduction

Silicene is a structural analog of graphene, exhibiting a two-dimensional matrix of silicon atoms, and because Si and C are in the same group in the periodical table with an s^2p^2 configuration of the valence electrons, they also display similar electronic properties, such as the "Dirac cone", high Fermi velocity and carrier mobility.[1] Yet, unlike graphene which is made up of sp^2-hybridized carbon atoms, silicon atoms adopt sp^3 hybridization in silicene, leading to a buckled hexagonal shape and a highly chemically active surface.[2,3] This provides opportunities for manipulating the dispersion of electrons, tuning the band gap, and enabling facile chemical functionalization of silicene.[2,3] The impacts of such structural engineering on the materials properties become increasingly pronounced for nanosized silicene. Note that its structural analog, graphene quantum dots (GQDs), have shown great potential for a wide range of applications, such as bioimaging, chemical sensing, therapeutics, drug delivery, photovoltaics, and catalysis.[4-15] It will therefore be of fundamental and technological significance to examine the properties and potential applications of the silicon counterparts, silicene quantum dots (SiQDs).

It has been a challenge in the preparation of silicon nanosheets, primarily because of the lack of natural silicon allotropes with a layered structure that renders it impossible to prepare silicene by mechanical stripping which has been used to fabricate many other 2D structures like graphene.[16,17] The chemical reduction method, which has also been used to convert graphene oxide to graphene, does not work for silicene synthesis either, because silicon oxide is chemically inert and structurally robust. So far, the leading method for silicene synthesis is by epitaxial growth on substrates such as Ag(110), Ag(001), Ag(111), Au(110), ZrB_2, ZrC(111), Ir(111) and MoS_2 surfaces, which necessitates sophisticated instrumentation and stringent experimental conditions.[18-25] Another effective strategy for silicene synthesis is by chemical exfoliation of metal silicide compounds (e.g., $MgSi_2$, and $CaSi_2$) by taking advantage of the hexagonal layered structure

consisting of alternating Mg or Ca layers and corrugated Si (111) planes in which the Si_6 rings are interconnected.[26,27] Regardless of the strategy that is adopted, further surface functionalization of the as-prepared silicene sheets is required so as to stabilize silicene in air and to provide a structural framework within which the physical, chemical and electronic properties of silicene can be deliberately manipulated for specific applications.[1]

In an early study,[27] Nakano *et al*. prepared organically stabilized few-layered silicon nanosheets of a few hundred nm across by hydrosilylation of layered polysilane (Si_6H_6) derived from chemical exfoliation of $CaSi_2$ single crystals. Hydrosilylation was carried out under relatively mild experimental conditions with 1-hexene, and yielded a densely packed organic monolayer on the silicon nanosheet surface which provided excellent protection against silicon oxidation. However, as H_2PtCl_6 was used as the hydrosilylation catalyst, Pt deposition might occur on the silicon nanosheet surface, and the contamination could impact the electronic and optical properties of the final product.[28,29] Therefore, an improved method and/or catalyst is required for the synthesis of high-quality silicene. Furthermore, by modifying the silicene surface with ligands that carry more complicated structures and chemical functional moieties (other than 1-hexene used in the previous study[27]), new optical and electronic properties may be imparted to the silicene nanosheets. This is the primary motivation of the present work.

In the present study we adopted a facile hydrothermal procedure to prepare organically stabilized SiQDs by using fine powders of $CaSi_2$ as raw materials, and PtO_2 powders, instead of H_2PtCl_4, as the hydrosilylation catalyst to minimize metal contamination.[30] The unique chemical reactivity of silicon hydride on the SiQD surface towards olefin and acetylene moieties forming Si–CH_2–CH_2– and Si–CH=CH– interfacial bonds was then exploited for the stabilization and functionalization of the SiQDs (Scheme 1).[31] Significantly the optical and electronic properties of SiQDs were found

to be readily engineered by the interfacial linkages, as manifested in photoluminescence and photoelectrochemical measurements.

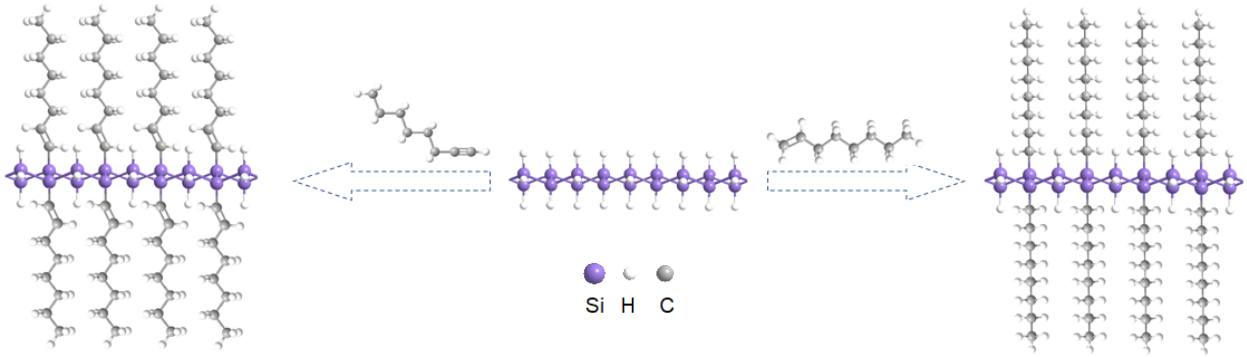

Scheme 1. Surface functionalization of SiQDs by (right) olefin and (left) acetylene derivatives.

Experimental Section

Chemicals. Calcium silicide ($CaSi_2$, Sigma Aldrich), 1-octyne (97%, ACROS), 1-octene (98%, Sigma Aldrich), vinylferrocene (VFc, 97%, ACROS), ethynylferrocene (EFc, 97 %, ACROS), chloroform-*d* ($CDCl_3$, 99.6%, ACROS), and hydrochloric acid (HCl, 12 M, Fisher Scientific) were all used as received. Solvents were purchased at the highest purity available from typical commercial sources and also used as received. Tetra-n-butylammonium perchlorate (TBAP, 98 %, TCI America) was used after recrystallization four times in ethanol. Water was supplied by a Barnstead Nanopure water system (18.3 MΩ·cm).

Sample preparation. SiQDs were prepared by adopting a procedure described in previous studies with some modifications.[27,32] In brief, 1 g of $CaSi_2$ powers was transferred to a 250 mL round bottom flask (A) in a glovebox, and 100 mL of concentrated HCl (12 M) was added to another 250 mL round-bottom flask (B), which was degassed with N_2 for 20 min. Both flasks were sealed and kept at –30 °C for 1 h before the solution from flask B was poured into flask A under N_2 protection. The mixture was sealed in flask A and kept at –30 °C for 14 d. SiQDs were collected

by centrifugation, rinsed with a copious amount of acetone, dried in vacuum at room temperature for 1 d, and stored in a sealed vial in the glovebox.

The obtained SiQDs were then functionalized with olefin and acetylene derivatives by a hydrothermal method.[30,33] To prepare acetylene-capped SiQDs, in a typical experiment, 29 mg of SiQDs, 2 mg of PtO_2 powders, and 3 mmol of 1-octyne dispersed in 10 mL of toluene were added into a 25 mL Teflon liner in the glovebox, which was then sealed in stainless steel autoclave and heated at 120 °C for 24 h. After being cooled down to room temperature, the content was filtered and the filtrate was condensed by rotary evaporation. The condensed solution was rinsed with copious acetonitrile to remove excess 1-octyne to yield purified 1-octyne-capped SiQDs (denoted as SiHC8). The same procedure was used to functionalize SiQDs with 1-octene, and the resulting sample was referred to as SiH2C8. Two additional samples were prepared where a mixture of 1-octyne (2 mmol) + EFc (1 mmol) or 1-octene (2 mmol) + VFc (1 mmol) was used, producing SiVFc and SiEFc, respectively.

Characterization. The morphology and sizes of SiQDs were characterized by atomic force microscopic (AFM, Molecular Imaging PicoLE SPM instrument) and transmission electron microscopic (TEM, Philips CM300 at 300 kV) measurements. The samples for AFM measurements were prepared by dropcasting a solution of the SiQD samples onto a freshly cleaved mica surface. Solvent evaporation at room temperature led to the deposition of SiQDs onto the mica surface. The topographic images were acquired under ambient conditions. X-ray photoelectron spectra (XPS) were recorded with a PHI 5400/XPS instrument equipped with an Al Kα source operated at 350 W and 10^{-9} Torr. UV-vis spectra were acquired with a Perkin-Elmer Lambda 35 UV-vis spectrometer by using a quartz cuvette (1 cm × 1 cm) as a sample container, and the same solutions were used for photoluminescence measurements with a FluoroMax-3

fluorospectrometer. ^{1}H NMR and ^{29}Si NMR spectroscopic measurements were carried out with a Varian Unity Inova 500 MHz NMR spectrometer with the samples dissolved in $CDCl_3$. In ^{29}Si NMR measurements, a Teflon NMR tube was used.

Electrochemistry. Voltammetric measurements were performed with a CHI 440 electrochemical workstation. A polycrystalline gold disk electrode sealed in a glass tubing was applied as working electrode. A Pt coil and a Ag/AgCl wire were used as the counter and (quasi)reference electrode, respectively. The gold electrode was first polished with aluminum oxide slurries (0.05 μm) and then cleaned by sonication in 0.1 HNO_3, H_2SO_4, and Nanopure water successively. Prior to data collection, the electrolyte solution (0.1 M TBAP in CH_2Cl_2) was deaerated with ultrahigh-purity N_2 for at least 20 min and blanketed with a nitrogen atmosphere during the entire experimental procedure. Square wave voltammograms (SWVs) were acquired both in the dark and under UV photoirradiation with a UV light source (256 nm, 6 W). The potentials were calibrated against the formal potential of ferrocene monomers (Fc^+/Fc) in the same electrolyte solution.

Results and Discussions

Figure 1 (A_1 and B_1) depicts two representative TEM images of SiQDs functionalized with 1-octene (SiH2C8). It can be seen that the SiQDs were well separated without apparent agglomeration (Figure $1A_1$), suggesting sufficient protection of the SiQDs by the 1-octene ligands, which reacted with Si–H on the SiQD surface forming Si–CH_2–CH_2–R interfacial bonds (Scheme 1 right). The formation of SiQDs is also evidenced in high-resolution TEM measurements (Figure $1B_1$), where well-defined lattice fringes can be seen with an interplanar spacing of 0.22 nm that is consistent with that of Si(211).[34] In addition, statistical analysis based on more than 300 nanoparticles shows that the majority of the SiQDs fell within the narrow range of 1.0 to 2.5 nm,

with an average diameter of 2.0 ± 0.5 nm, as evidenced in the core-size histogram in the inset to panel (B_1). Consistent results were obtained with SiQDs capped with other organic ligands. AFM topographic measurements (Figure $1A_2$ and $1B_2$) also showed good dispersion of the SiQDs, of which the thickness was estimated by line scans to be 3.5 – 3.6 nm (Figure $1A_3$ and $1B_3$). Considering the fully extended chainlength of an octyl ligand is 0.89 nm (by Hyperchem®

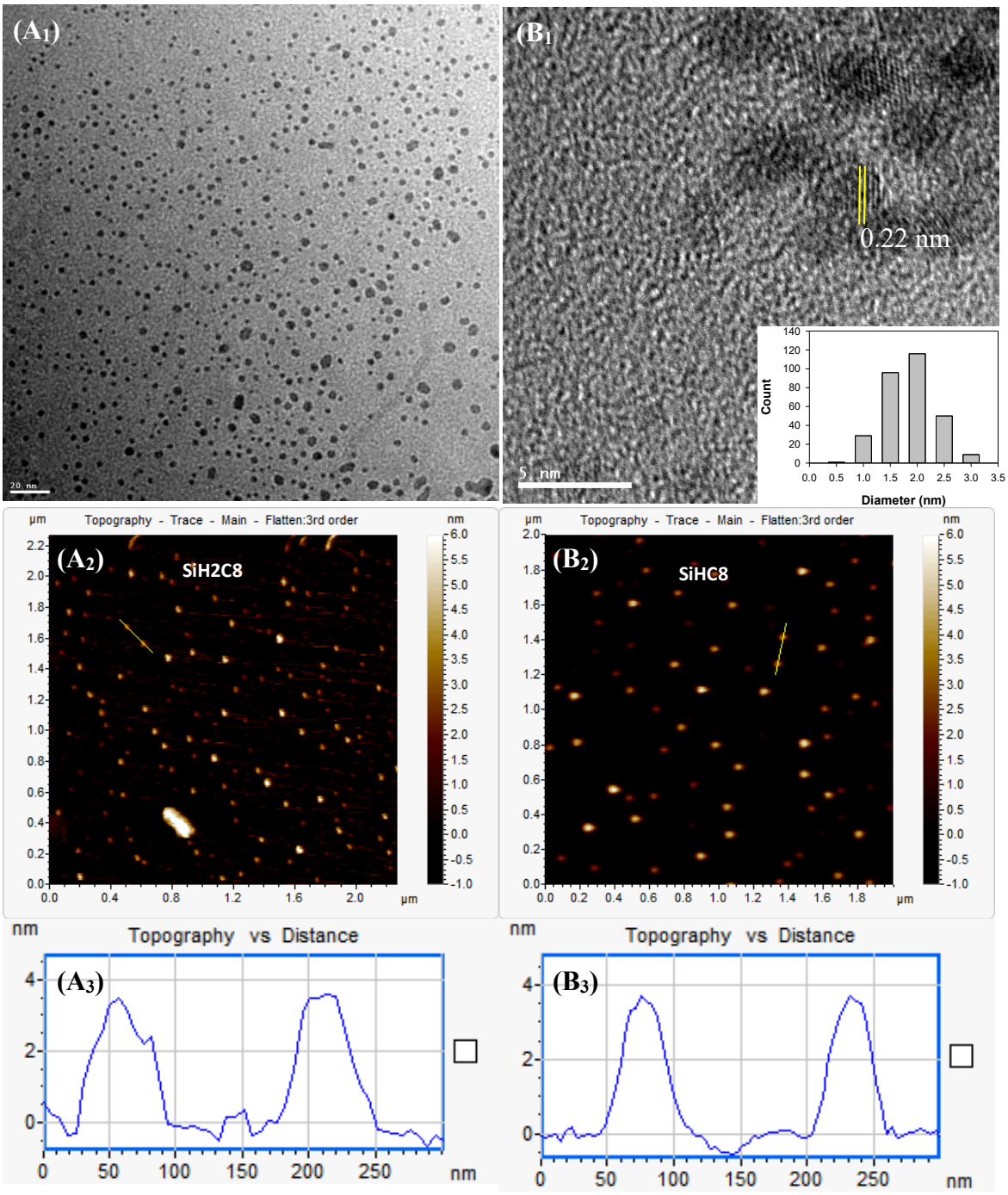

calculation), this suggests that the thickness of a SiQD is about 1.6 nm, corresponding to *ca*. 4 atomic layers of silicon.[35]

Figure 1. (A_1, B_1) Representative TEM images of SiH2C8. Scale bars are 20 nm in (A_1) and 5 nm in (B_1). Inset to panel (B_1) is the core size histogram. AFM topographs of (A_2) SiH2C8 and (B_2) SiHC8, with the height profiles in the corresponding line scans depicted in panels (A_3) and (B_3), respectively.

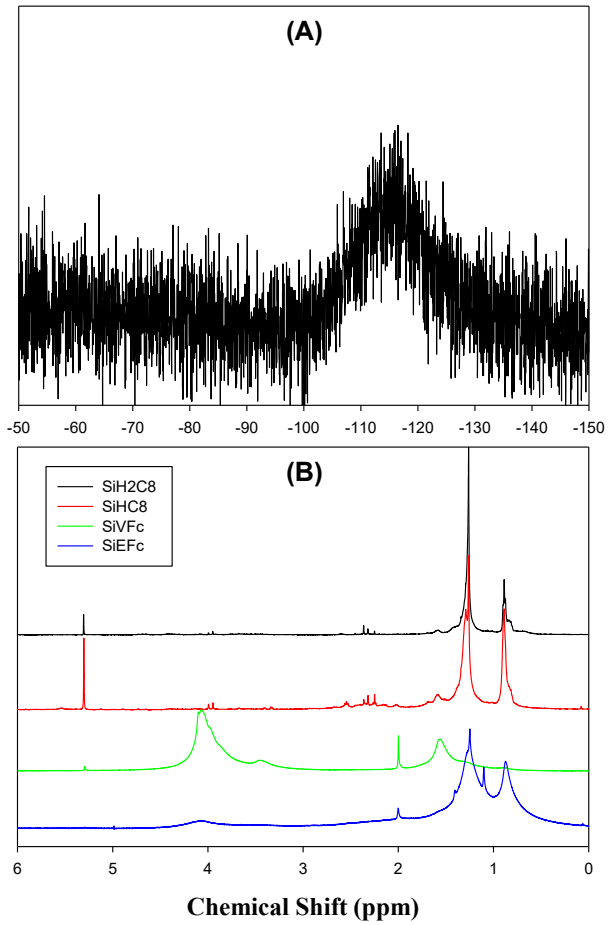

Figure 2. (A) ^{29}Si NMR spectrum of SiH2C8, and (B) ^{1}H NMR spectra of SiH2C8, SiHC8, SiVFc, and SiEFc in $CDCl_3$.

The structure of SiQDs was further examined by NMR measurements. Figure 2A depicts the ^{29}Si NMR spectrum for SiH2C8. One can see that within the range of –50 to –150 ppm with respect to TMS, a single broad peak emerged at –112 ppm. This may be assigned to silicon atoms bonded

to two or three other silicon atoms in a silane-like structure,[36,37] consistent with the few-layered structure of the SiQD samples. In ^{1}H NMR measurements (Figure 2B), two broad peaks can be observed at 0.88 and 1.27 ppm with SiH2C8, due to the terminal methyl protons and methylene protons of the aliphatic chains, confirming the successful functionalization of SiQDs by the 1-octene ligands. Consistent results were obtained with the SiHC8 sample. For the SiVFc and SiEFc samples, two additional broad bands appear at 4.05 and 3.46 ppm, arising from the ferrocenyl ring protons, and according to the integrated peak areas, the surface coverage of the ferrocenyl moieties was estimated to be 74% and 37% for SiVFc and SiEFc, respectively. The discrepancy of the ferrocene surface coverage might be due to the more rigid interfacial linkage and tightly packed capping layer in SiEFc that made it sterically challenging to accommodate the bulky ferrocene moiety (Scheme 1). Importantly, the fact that only broad peaks were observed indicates the successful attachment of the functional moieties onto the SiQD surface and the samples were spectroscopically clean without any excess ligands (note that the sharp peaks at around 5.27, 2.00, and 1.56 ppm are due to residual solvents of chloroform, acetonitrile, and water, respectively).[38]

The chemical composition and valence state of Si in SiH2C8 and SiHC8 were then determined by XPS measurements. From the survey spectra in Figure 3A one can see that both SiH2C8 and SiHC8 exhibited four peaks at 101.6 eV, 152.6 eV, 284.0 eV, and 531.3 eV, due to Si 2p, Si 2s, C 1s and O 1s electrons, respectively.[39] No other elements can be identified, again, indicating that the samples were spectroscopically clean (e.g., no Pt residual). In the high-resolution scans in Figure 3B, both samples show a single peak at almost the same binding energy of 101.32 and 101.22 eV for the Si 2p electrons, which fell in the intermediate between those for bulk Si (99.15 eV) and SiO_2 (103.4 eV),[39] consistent with the formation of few-layered SiQDs.[27,40]

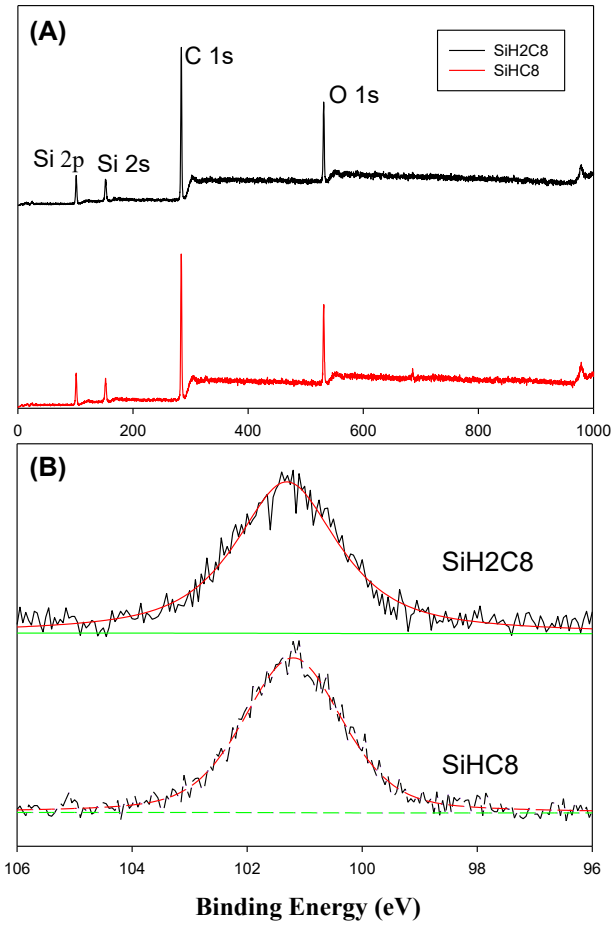

Figure 3. (A) XPS survey spectra and (B) high-resolution scans of the Si 2p electrons of SiH2C8 and SiHC8. In panel (B), black curves are experimental data and colored curves are deconvolution fits.

The optical properties of the organically functionalized SiQDs were then characterized by UV-vis and photoluminescence measurements. As shown in Figure 4A, all the samples exhibited a largely exponential decay profile in UV-vis absorption measurements, in agreement with the formation of SiQDs.[41-43] Additionally, a shoulder band (marked by asterisks) can be identified at around 320 nm for both SiH2C8 (black curve) and SiHC8 (red curve), which may be ascribed to the interband transition of two-dimensional honeycomb silicene.[44] Furthermore, for SiVFc (green curve) one may identify another broad band (#) at around 458 nm, due to the absorption of SiQD-

bound ferrocene moieties; note that this peak was much weaker for SiEFc (blue curve), likely because of a lower surface concentration of the ferrocene groups (Figure 2).[45]

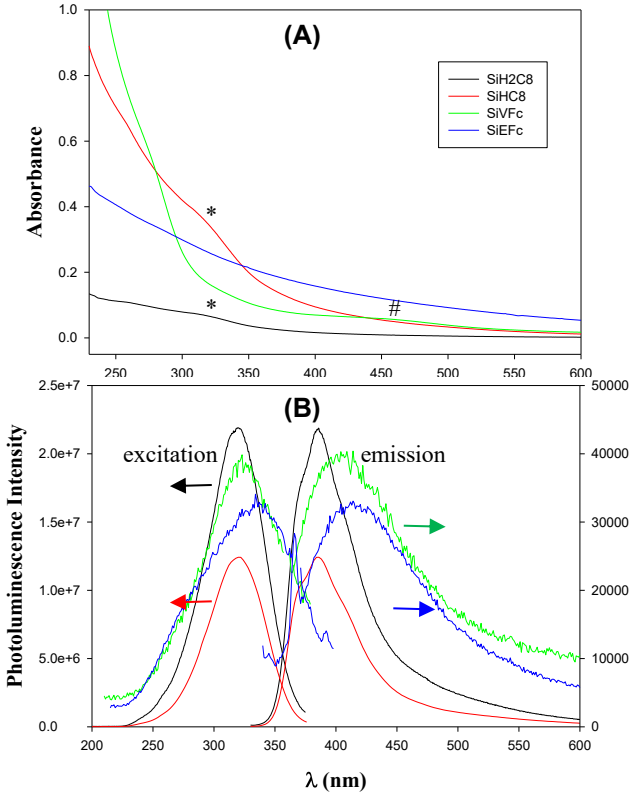

Figure 4. (A) UV-vis and (B) photoluminescence spectra of SiQDs capped with varied organic ligands in $CHCl_3$. In panel (B), the photoluminescence intensity was normalized to the optical density at the excitation peak position obtained from panel (A).

Consistent results were obtained in photoluminescence measurements. As show in Figure 4B, all four samples exhibited apparent photoluminescence emissions. It is clear that both SiH2C8 and SiHC8 displayed very strong photoluminescence with the excitation and emission peaks at 320 and 385 nm, respectively. This corresponds to a bandgap of ca. 2.95 eV, markedly higher than that of bulk silicon (1.1 eV),[46] but close to the theoretical value of the direct bandgap of layered polysilane (Si_6H_6, 3 eV),[27,47] most likely due to quantum confinement effects — note that the size of the SiQDs prepared above (Figure 1) is markedly smaller than the exciton Bohr radius of silicon

(~ 5 nm).[48] Furthermore, the normalized photoluminescence emission of SiH2C8 was apparently stronger than that of SiHC8, likely because of quenching by the unsaturated Si–CH=CH– interfacial linkage in SiHC8, as compared to the saturated Si–CH_2–CH_2– in SiH2C8.[49-52] Furthermore, the photoluminescence excitation and emission of SiVFc and SiEFc showed a slight red-shift with much reduced intensity. Specifically, SiVFc displayed the excitation and emission maxima at 325 and 406 nm, respectively, and the emission intensity was *ca*. 540 times weaker than that of SiH2C8, whereas the excitation and emission peaks for SiEFc red-shifted further to 336 and 415 nm, and the emission intensity was even lower, 650 times weaker than that of SiHC8. These observations may be accounted for by the quenching effect of the ferrocenyl moieties where the unsaturated interfacial bonds further facilitated electron transfer from the SiQDs to the surface ligands.

Both ferrocene-functionalized SiVFc and SiEFc also exhibit interesting photoelectrochemical properties. From the square-wave voltammograms (SWVs) in Figure 5, one can see that SiEFc exhibits a pair of broad voltammetric peaks (black curve) between –0.2 and +0.4 V in the dark, with a formal potential of E°' = +0.15 V (vs Fc^+/Fc). This is most likely due to the redox reaction of the ferrocene moieties, Fc ↔ Fc^+ + e. Yet, the peak width at half maximum (~400 mV) is markedly larger than that expected of a reversible single-electron transfer reaction (90.5 mV),[53] suggesting energy differentiation among the SiQD-bound ferrocene moieties, likely due to an inhomogeneous spatial distribution of ferrocene on the two-dimensional silicene surface (Scheme 1). Such effects have been observed in earlier studies with two-dimensional self-assembled monolayers of ferrocene derivatives on gold.[54] Very consistent voltammetric features were observed when the measurements were carried out under UV photoirradiation (λ = 256 nm, red curve), except that an additional pair of voltammetric peaks emerged at a negative potential E°' =

–0.41 V. For comparison, the SiHC8 sample exhibited only featureless voltammetric profiles under the same UV photoirradiation (blue curve, which is almost invariant to that in the dark, not shown). This suggests that the ferrocene moieties were responsible for the voltammetric peak at –0.41 V, likely due to the oxidation and reduction of ferrocene anions, $Fc^- \leftrightarrow Fc + e$. In a prior study,[55] the energy difference between ferrocene and ferrocene anion was estimated to be 0.427 eV by DFT calculations, very comparable to the potential difference (0.56 V) observed here between the two pairs of voltammetric peaks. In the present study, the formation of ferrocene anion is likely a result of photoinduced electron transfer from silicene to the ferrocene metal center, and the fact that the peak current of ferrocene anion is markedly lower than that of $Fc \leftrightarrow Fc^+ + e$ suggests only a small fraction of the ferrocene moieties were photo-reduced. This is consistent with the apparent quenching of the silicene photoluminescence upon the functionalization by the ferrocene ligands, as observed above in Figure 4. To the best of our knowledge, this is the first ever experimental observation of ferrocene anions produced by photoinduced charge transfer.

Similar photoelectrochemical characteristics were observed with the SiVFc sample, except that the voltammetric peak currents for the negative peak under UV photoirradiation were much lower (Figure S1), indicating an even lower ferrocene anion concentration, despite a higher ferrocene coverage on the SiQD surface (Figure 2). This may be accounted for, at least in part, by the difference of the interfacial bonding interactions.[56,57] In SiEFc, the ferrocene groups were attached onto silicene by an unsaturated Si–CH=CH–Fc linkage, whereas a saturated interfacial bond was formed in SiVFc, $Si–CH_2–CH_2–Fc$. The latter is anticipated to impede charge transfer from silicene to the ferrocene metal centers.

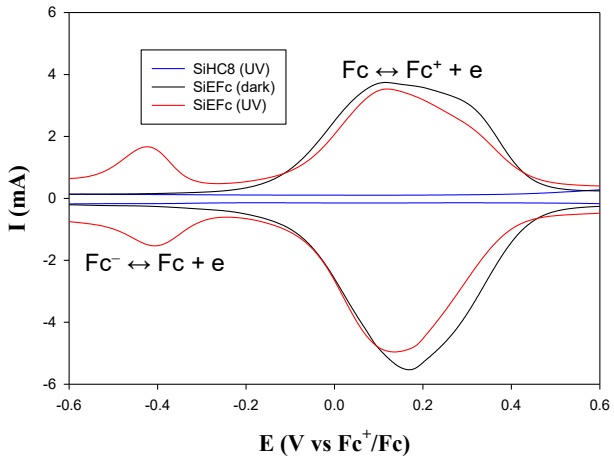

Figure 5. Square-wave voltammograms (SWVs) of SiEFc in 0.1 M TBAP in CH_2Cl_2. Electrode surface area ca. 2 mm^2. SiQD concentrations 5 mg/mL for SiEFc, and 5 mg/mL for SiHC8. Potential increment 2 mV, pulse amplitude 25 mV, and frequency 15 Hz.

Conclusions

SiQDs was derived from $CaSi_2$ and further functionalized with aliphatic ligands by taking advantage of the unique chemical reactivity of silicon hydride with olefin and acetylene moieties forming Si–CH_2–CH_2– and Si–CH=CH– interfacial linkages. TEM and AFM topographic measurements showed that the obtained SiQDs were about 2 nm in diameter and consisted of ca. 4 atomic layers of silicon. Spectroscopic measurements, such as ^{1}H and ^{29}Si NMR and XPS, confirmed the successful formation of SiQDs and the surface functionalization by aliphatic ligands. The obtained SiQDs exhibited apparent photoluminescence, with the emission intensity varied with the surface capping ligands. In comparison with SiH2C8, SiHC8 exhibited markedly quenched emission, and even more pronounced quenching was observed with SiVFc and SiEFc, likely due to electron transfer from SiQD to the surface capping ligands. Interestingly, both SiEFc and SiVFc exhibited unique photoelectrochemical properties with an additional pair of voltammetric peaks at a negative potential position under UV photoirradiation, in comparison to results in the dark, which suggests the formation of ferrocene anions, likely due to photoinduced

electron transfer from SiQD to the ferrocene metal centers, in good agreement with the quenching of the SiQD photoluminescence.

ASSOCIATED CONTENT

Supporting Information. The following file is available free of charge, SWVs of SiVFc.

AUTHOR INFORMATION

Corresponding Author

* shaowei@ucsc.edu

Author Contributions

The manuscript was written through contributions of all authors. All authors have given approval to the final version of the manuscript.

ACKNOWLEDGMENT

This work was supported, in part, by the National Science Foundation (DMR-1409396 and CHE-1710408). TEM and XPS work was carried out at the National Center for Electron Microscopy and Molecular Foundry of Lawrence Berkeley National Laboratory, which is supported by the US Department of Energy.

REFERENCES

(1) Zhao, J. J.; Liu, H. S.; Yu, Z. M.; Quhe, R. G.; Zhou, S.; Wang, Y. Y.; Liu, C. C.; Zhong, H. X.; Han, N. N.; Lu, J.; Yao, Y. G.; Wu, K. H. Rise of silicene: A competitive 2D material. *Prog Mater Sci* **2016**, *83*, 24-151.

(2) Du, Y.; Zhuang, J. C.; Liu, H. S.; Xu, X.; Eilers, S.; Wu, K. H.; Cheng, P.; Zhao, J. J.; Pi, X. D.; See, K. W.; Peleckis, G.; Wang, X. L.; Dou, S. X. Tuning the Band Gap in Silicene by Oxidation. *Acs Nano* **2014**, *8*, 10019-10025.

(3) Jose, D.; Datta, A. Structures and Chemical Properties of Silicene: Unlike Graphene. *Acc Chem Res* **2014**, *47*, 593-602.

(4) Zhu, S. J.; Song, Y. B.; Wang, J.; Wan, H.; Zhang, Y.; Ning, Y.; Yang, B. Photoluminescence mechanism in graphene quantum dots: Quantum confinement effect and surface/edge state. *Nano Today* **2017**, *13*, 10-14.

(5) Jin, S. H.; Kim, D. H.; Jun, G. H.; Hong, S. H.; Jeon, S. Tuning the Photoluminescence of Graphene Quantum Dots through the Charge Transfer Effect of Functional Groups. *Acs Nano* **2013**, *7*, 1239-1245.

(6) Song, S. H.; Jang, M.; Yoon, H.; Cho, Y. H.; Jeon, S.; Kim, B. H. Size and pH dependent photoluminescence of graphene quantum dots with low oxygen content. *Rsc Adv* **2016**, *6*, 97990-97994.

(7) Hwang, E.; Hwang, H. M.; Shin, Y.; Yoon, Y.; Lee, H.; Yang, J.; Bak, S.; Lee, H. Chemically modulated graphene quantum dot for tuning the photoluminescence as novel sensory probe. *Sci Rep-Uk* **2016**, *6*, 39448.

(8) Deng, X. X.; Sun, J.; Yang, S. W.; Shen, H.; Zhou, W.; Lu, J.; Ding, G. Q.; Wang, Z. Y. The emission wavelength dependent photoluminescence lifetime of the N-doped graphene quantum dots. *Appl Phys Lett* **2015**, *107*, 241905.

(9) Shen, J. H.; Zhu, Y. H.; Yang, X. L.; Li, C. Z. Graphene quantum dots: emergent nanolights for bioimaging, sensors, catalysis and photovoltaic devices. *Chem Commun* **2012**, *48*, 3686-3699.

(10) Ge, J. C.; Lan, M. H.; Zhou, B. J.; Liu, W. M.; Guo, L.; Wang, H.; Jia, Q. Y.; Niu, G. L.; Huang, X.; Zhou, H. Y.; Meng, X. M.; Wang, P. F.; Lee, C. S.; Zhang, W. J.; Han, X. D. A graphene quantum dot photodynamic therapy agent with high singlet oxygen generation. *Nat Commun* **2014**, *5*, 4596.

(11) Iannazzo, D.; Pistone, A.; Salamo, M.; Galvagno, S.; Romeo, R.; Giofre, S. V.; Branca, C.; Visalli, G.; Di Pietro, A. Graphene quantum dots for cancer targeted drug delivery. *Int J Pharmaceut* **2017**, *518*, 185-192.

(12) Sun, H. J.; Wu, L.; Wei, W. L.; Qu, X. G. Recent advances in graphene quantum dots for sensing. *Mater Today* **2013**, *16*, 433-442.

(13) Son, D. I.; Kwon, B. W.; Park, D. H.; Seo, W. S.; Yi, Y.; Angadi, B.; Lee, C. L.; Choi, W. K. Emissive ZnO-graphene quantum dots for white-light-emitting diodes. *Nat Nanotechnol* **2012**, *7*, 465-471.

(14) Guo, C. X.; Yang, H. B.; Sheng, Z. M.; Lu, Z. S.; Song, Q. L.; Li, C. M. Layered Graphene/Quantum Dots for Photovoltaic Devices. *Angew Chem Int Edit* **2010**, *49*, 3014-3017.

(15) Hu, P. G.; Liu, K.; Deming, C. P.; Chen, S. W. Multifunctional graphene-based nanostructures for efficient electrocatalytic reduction of oxygen. *J Chem Technol Biotechnol* **2015**, *90*, 2132-2151.

(16) Novoselov, K. S.; Geim, A. K.; Morozov, S. V.; Jiang, D.; Zhang, Y.; Dubonos, S. V.; Grigorieva, I. V.; Firsov, A. A. Electric field effect in atomically thin carbon films. *Science* **2004**, *306*, 666-669.

(17) Novoselov, K. S.; Jiang, D.; Schedin, F.; Booth, T. J.; Khotkevich, V. V.; Morozov, S. V.; Geim, A. K. Two-dimensional atomic crystals. *P Natl Acad Sci USA* **2005**, *102*, 10451-10453.

(18) Leandri, C.; Oughaddou, H.; Aufray, B.; Gay, J. M.; Le Lay, G.; Ranguis, A.; Garreau, Y. Growth of Si nanostructures on Ag(001). *Surf Sci* **2007**, *601*, 262-267.

(19) Aufray, B.; Kara, A.; Vizzini, S.; Oughaddou, H.; Leandri, C.; Ealet, B.; Le Lay, G. Graphene-like silicon nanoribbons on Ag(110): A possible formation of silicene. *Appl Phys Lett* **2010**, *96*, 183102.

(20) Tchalala, M. R.; Enriquez, H.; Mayne, A. J.; Kara, A.; Roth, S.; Silly, M. G.; Bendounan, A.; Sirotti, F.; Greber, T.; Aufray, B.; Dujardin, G.; Ali, M. A.; Oughaddou, H. Formation of one-dimensional self-assembled silicon nanoribbons on Au(110)-(2 x 1). *Appl Phys Lett* **2013**, *102*, 083107.

(21) Vogt, P.; De Padova, P.; Quaresima, C.; Avila, J.; Frantzeskakis, E.; Asensio, M. C.; Resta, A.; Ealet, B.; Le Lay, G. Silicene: Compelling Experimental Evidence for Graphenelike Two-Dimensional Silicon. *Phys Rev Lett* **2012**, *108*, 155501.

(22) Fleurence, A.; Friedlein, R.; Ozaki, T.; Kawai, H.; Wang, Y.; Yamada-Takamura, Y. Experimental Evidence for Epitaxial Silicene on Diboride Thin Films. *Phys Rev Lett* **2012**, *108*.

(23) Aizawa, T.; Suehara, S.; Otani, S. Silicene on Zirconium Carbide (111). *J Phys Chem C* **2014**, *118*, 23049-23057.

(24) Meng, L.; Wang, Y. L.; Zhang, L. Z.; Du, S. X.; Wu, R. T.; Li, L. F.; Zhang, Y.; Li, G.; Zhou, H. T.; Hofer, W. A.; Gao, H. J. Buckled Silicene Formation on Ir(111). *Nano Lett* **2013**, *13*, 685-690.

(25) Chiappe, D.; Scalise, E.; Cinquanta, E.; Grazianetti, C.; van den Broek, B.; Fanciulli, M.; Houssa, M.; Molle, A. Two-Dimensional Si Nanosheets with Local Hexagonal Structure on a MoS2 Surface. *Adv Mater* **2014**, *26*, 2096-2101.

(26) Nakano, H.; Mitsuoka, T.; Harada, M.; Horibuchi, K.; Nozaki, H.; Takahashi, N.; Nonaka, T.; Seno, Y.; Nakamura, H. Soft synthesis of single-crystal silicon monolayer sheets. *Angew Chem Int Edit* **2006**, *45*, 6303-6306.

(27) Nakano, H.; Nakano, M.; Nakanishi, K.; Tanaka, D.; Sugiyama, Y.; Ikuno, T.; Okamoto, H.; Ohta, T. Preparation of Alkyl-Modified Silicon Nanosheets by Hydrosilylation of Layered Polysilane (Si6H6). *J Am Chem Soc* **2012**, *134*, 5452-5455.

(28) Holland, J. M.; Stewart, M. P.; Allen, M. J.; Buriak, J. M. Metal mediated reactions on porous silicon surfaces. *J Solid State Chem* **1999**, *147*, 251-258.

(29) Purkait, T. K.; Iqbal, M.; Wahl, M. H.; Gottschling, K.; Gonzalez, C. M.; Islam, M. A.; Veinot, J. G. C. Borane-Catalyzed Room-Temperature Hydrosilylation of Alkenes/Alkynes on Silicon Nanocrystal Surfaces. *J Am Chem Soc* **2014**, *136*, 17914-17917.

(30) Sabourault, N.; Mignani, G.; Wagner, A.; Mioskowski, C. Platinum oxide (PtO2): A potent hydrosilylation catalyst. *Org Lett* **2002**, *4*, 2117-2119.

(31) Peng, Y.; Deming, C. P.; Chen, S. W. Intervalence Charge Transfer Mediated by Silicon Nanoparticles. *Chemelectrochem* **2016**, *3*, 1219-1224.

(32) Sugiyama, Y.; Okamoto, H.; Mitsuoka, T.; Morikawa, T.; Nakanishi, K.; Ohta, T.; Nakano, H. Synthesis and Optical Properties of Monolayer Organosilicon Nanosheets. *J Am Chem Soc* **2010**, *132*, 5946-+.

(33) Yang, Z. Y.; Iqbal, M.; Dobbie, A. R.; Veinot, J. G. C. Surface-Induced Alkene Oligomerization: Does Thermal Hydrosilylation Really Lead to Monolayer Protected Silicon Nanocrystals? *J Am Chem Soc* **2013**, *135*, 17595-17601.

(34) Tilley, R. D.; Warner, J. H.; Yamamoto, K.; I, M.; Fujimori, H. Micro-emulsion synthesis of monodisperse surface stabilized silicon nanocrystals. *Chem Commun* **2005**, 1833-1835.

(35) Tao, L.; Cinquanta, E.; Chiappe, D.; Grazianetti, C.; Fanciulli, M.; Dubey, M.; Molle, A.; Akinwande, D. Silicene field-effect transistors operating at room temperature. *Nat Nanotechnol* **2015**, *10*, 227-231.

(36) Heine, T.; Goursot, A.; Seifert, G.; Webert, J. Performance of DFT for Si-29 NMR chemical shifts of silanes. *J Phys Chem A* **2001**, *105*, 620-626.

(37) Luhmer, M.; dEspinose, J. B.; Hommel, H.; Legrand, A. P. High-resolution Si-29 solid-state NMR study of silicon functionality distribution on the surface of silicas. *Magn Reson Imaging* **1996**, *14*, 911-913.

(38) Hostetler, M. J.; Wingate, J. E.; Zhong, C. J.; Harris, J. E.; Vachet, R. W.; Clark, M. R.; Londono, J. D.; Green, S. J.; Stokes, J. J.; Wignall, G. D.; Glish, G. L.; Porter, M. D.; Evans, N. D.; Murray, R. W. Alkanethiolate gold cluster molecules with core diameters from 1.5 to 5.2 nm: Core and monolayer properties as a function of core size. *Langmuir* **1998**, *14*, 17-30.

(39) Wagner, C. D.; Riggs, W. M.; Davis, L. E.; Moulder, J. F.; Muilenberg, G. E.: *Handbook of x-ray photoelectron spectroscopy : a reference book of standard data for use in x-ray photoelectron spectroscopy*; Perkin-Elmer Corp.: Eden Prairie, Minn., 1979.

(40) Mastronardi, M. L.; Hennrich, F.; Henderson, E. J.; Maier-Flaig, F.; Blum, C.; Reichenbach, J.; Lemmer, U.; Kubel, C.; Wang, D.; Kappes, M. M.; Ozin, G. A. Preparation of Monodisperse Silicon Nanocrystals Using Density Gradient Ultracentrifugation. *J Am Chem Soc* **2011**, *133*, 11928-11931.

(41) Kuznetsov, A. I.; Miroshnichenko, A. E.; Fu, Y. H.; Zhang, J. B.; Luk'yanchuk, B. Magnetic light. *Sci Rep-Uk* **2012**, *2*, 492.

(42) Garcia-Camara, B.; Algorri, J. F.; Urruchi, V.; Sanchez-Pena, J. M. Directional Scattering of Semiconductor Nanoparticles Embedded in a Liquid Crystal. *Materials* **2014**, *7*, 2784-2794.

(43) Kuznetsov, A. I.; Miroshnichenko, A. E.; Brongersma, M. L.; Kivshar, Y. S.; Luk'yanchuk, B. Optically resonant dielectric nanostructures. *Science* **2016**, *354,* 846.

(44) Matthes, L.; Pulci, O.; Bechstedt, F. Optical properties of two-dimensional honeycomb crystals graphene, silicene, germanene, and tinene from first principles. *New J Phys* **2014**, *16*, 105007.

(45) Sohn, Y. S.; Hendrick.Dn; Gray, H. B. Electronic Structure of Metallocenes. *J Am Chem Soc* **1971**, *93*, 3603-&.

(46) Wilcoxon, J. P.; Samara, G. A.; Provencio, P. N. Optical and electronic properties of Si nanoclusters synthesized in inverse micelles. *Physical Review B* **1999**, *60*, 2704-2714.

(47) He, J.; Tse, J. S.; Klug, D. D.; Preston, K. F. Layered polysilane: thermolysis and photoluminescence. *J Mater Chem* **1998**, *8*, 705-710.

(48) Kole, A.; Chaudhuri, P. Growth of silicon quantum dots by oxidation of the silicon nanocrystals embedded within silicon carbide matrix. *AIP Adv* **2014**, *4*, 107106.

(49) de Silva, A. P.; Gunaratne, H. Q. N.; Gunnlaugsson, T. Fluorescent PET (photoinduced electron transfer) reagents for thiols. *Tetrahedron Lett* **1998**, *39*, 5077-5080.

(50) Mabire, A. B.; Robin, M. P.; Quan, W. D.; Willcock, H.; Stavros, V. G.; O'Reilly, R. K. Aminomaleimide fluorophores: a simple functional group with bright, solvent dependent emission. *Chem Commun* **2015**, *51*, 9733-9736.

(51) Guy, J.; Caron, K.; Dufresne, S.; Michnick, S. W.; Skene, W. G.; Keillor, J. W. Convergent preparation and photophysical characterization of dimaleimide dansyl fluorogens: Elucidation of the maleimide fluorescence quenching mechanism. *J Am Chem Soc* **2007**, *129*, 11969-11977.

(52) Youziel, J.; Akhbar, A. R.; Aziz, Q.; Smith, M. E. B.; Caddick, S.; Tinker, A.; Baker, J. R. Bromo- and thiomaleimides as a new class of thiol-mediated fluorescence 'turn-on' reagents. *Org Biomol Chem* **2014**, *12*, 557-560.

(53) Ramaley, L.; Krause, M. S. Theory of Square Wave Voltammetry. *Anal Chem* **1969**, *41*, 1362-1365.

(54) Chidsey, C. E. D.; Bertozzi, C. R.; Putvinski, T. M.; Mujsce, A. M. Coadsorption of Ferrocene-Terminated and Unsubstituted Alkanethiols on Gold - Electroactive Self-Assembled Monolayers. *J Am Chem Soc* **1990**, *112*, 4301-4306.

(55) Ricke, N.; Eustis, S. N.; Bowen, K. H. Combined experimental and theoretical study of deprotonated ferrocene: Anion photoelectron spectroscopy and density functional calculations. *Int J Mass Spectr* **2014**, *357*, 63-65.

(56) Hoffmann, R. Interaction of Orbitals through Space and through Bonds. *Acc Chem Res* **1971**, *4*, 1-&.

(57) Quardokus, R. C.; Lu, Y. H.; Wasio, N. A.; Lent, C. S.; Justaud, F.; Lapinte, C.; Kandel, S. A. Through-Bond versus Through-Space Coupling in Mixed-Valence Molecules: Observation of Electron Localization at the Single-Molecule Scale. *J Am Chem Soc* **2012**, *134*, 1710-1714.

ToC Graph